

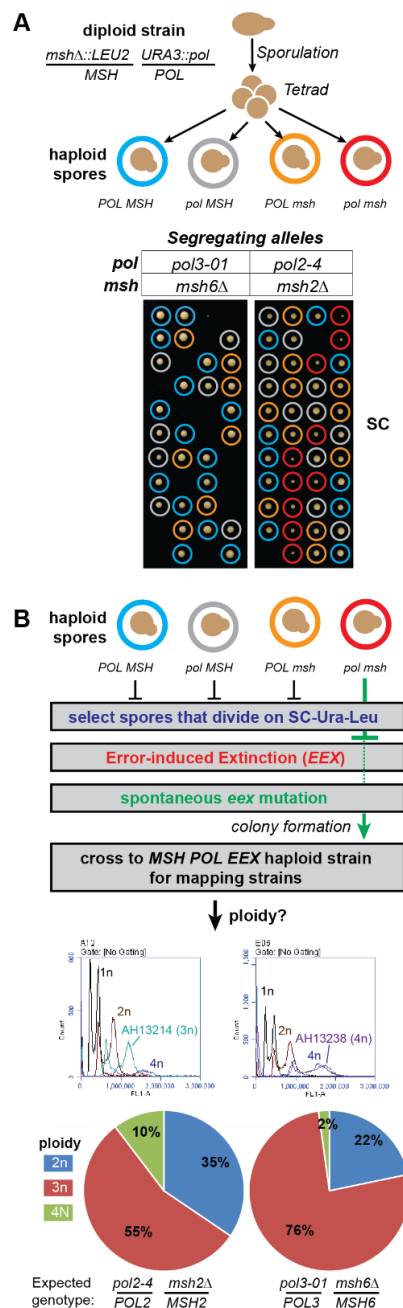
Spontaneous polyploids and antimutators compete during the evolution of *Saccharomyces cerevisiae* mutator cells

Maxwell A. Tracy, Mitchell B. Lee, Brady L. Hearn, Ian T. Dowsett, Luke C. Thurber, Jason Loo, Anisha M. Loeb, Kent Preston, Miles I. Tuncel, Niloufar Ghodsian, Anna Bode, Thao T. Tang, Andy R. Chia, and Alan J. Herr*

Department of Pathology, University of Washington, Seattle, Washington 98195

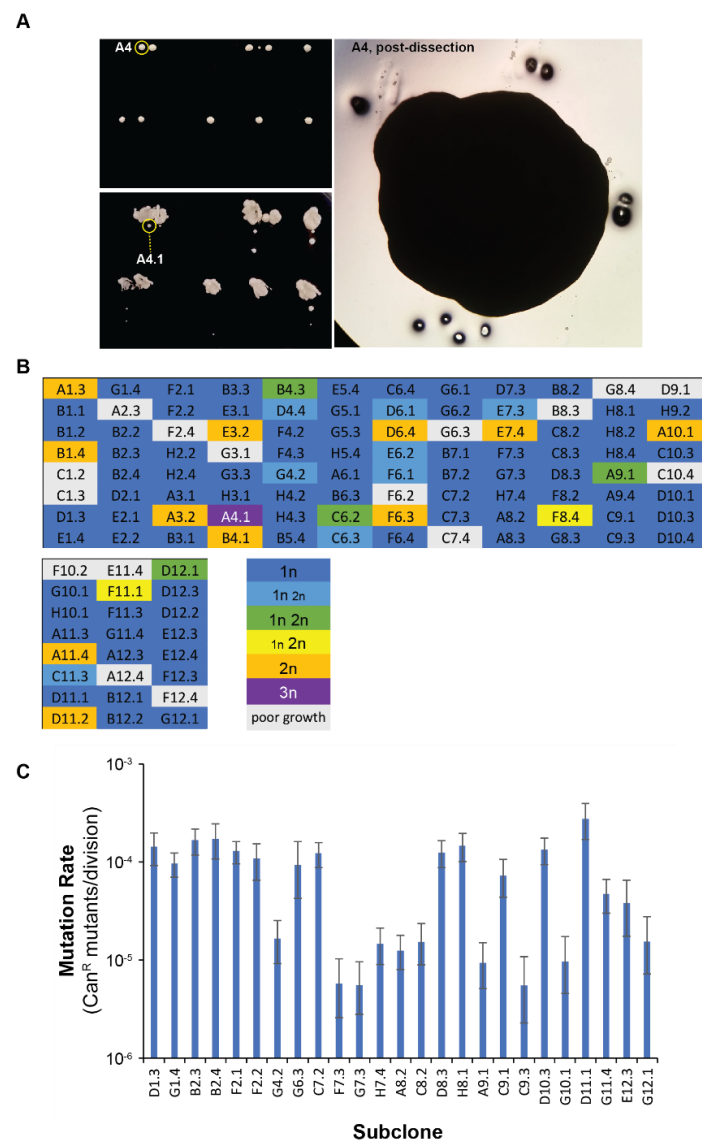
Supplementary Information

Figure S1. Discovery of spontaneous polyploid eex mutants.



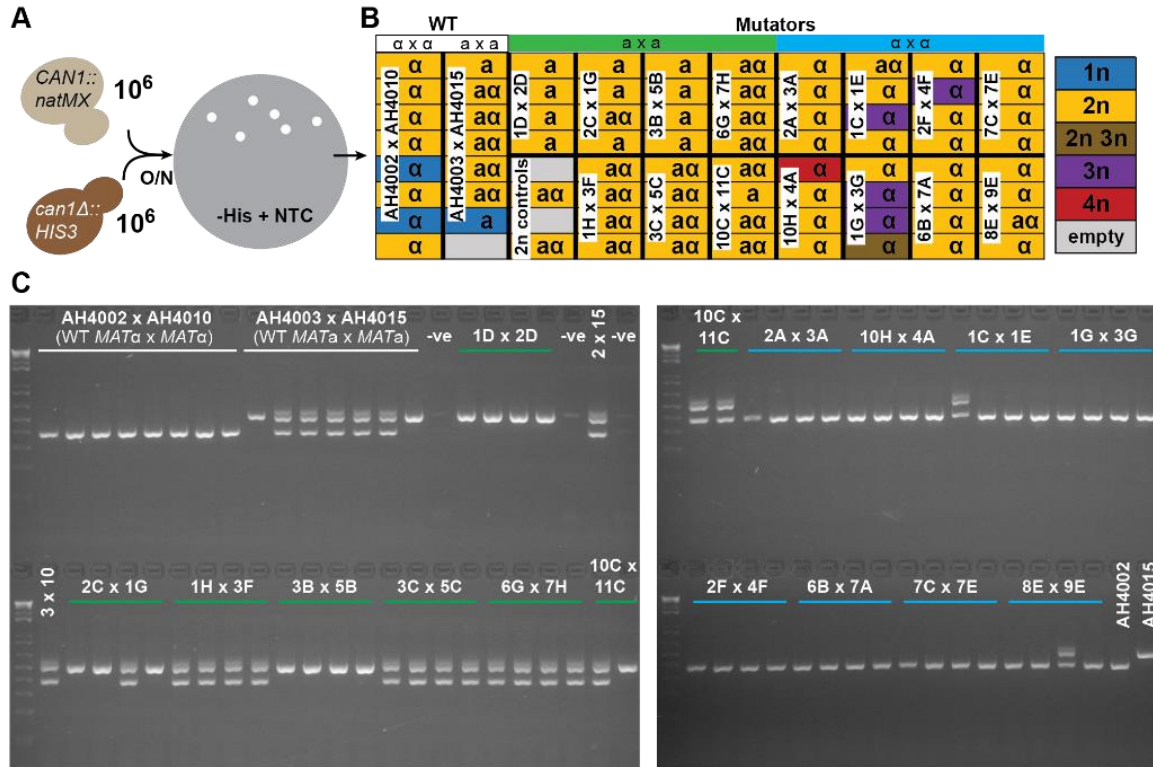
A) Synthetic growth phenotypes of freshly dissected *pol3-01 msh6Δ* and *pol2-4 msh2Δ* spore clones. *Top*, Schematic of strain genotypes and tetrad dissections. *Bottom*, Images of tetrad dissections after 48 hours of growth. Colored circles indicate genotypes. B) Isolation of *eex* mutants and evidence for polyploidization. *Top*, Scheme for isolating *eex* mutants and the generation of mapping strains. *Bottom*, Flow cytometry traces of two representative polyploid strains (AH13214 and AH13238; see Dataset 1) and 1n, 2n, and 4n controls as well as tally of the ploidies of the mapping strains.

Figure S2. Polyploids and antimutator subclones emerge with similar frequencies during the evolution of *pol2-4 msh2Δ* cultures.



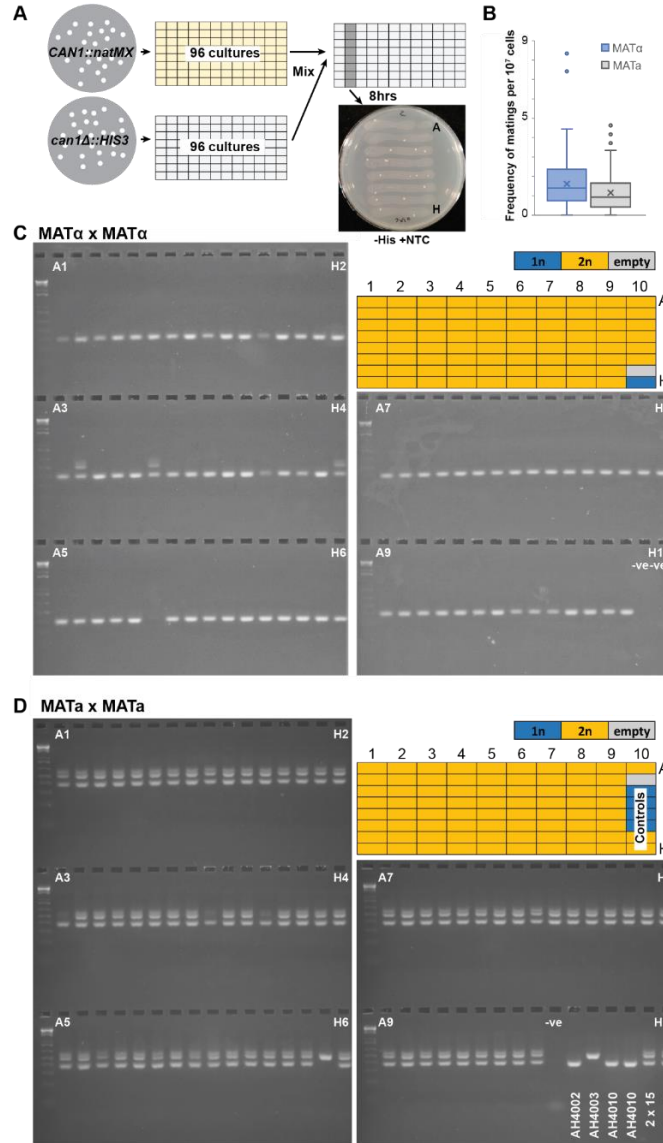
A) Representative images of colonies. *Clockwise from the top left*: initial colonies after 24 hours, A4 (a mixture of 1n and 3n cells) is circled in yellow; close-up of A4 just after removing single cells from the perimeter (holes were punched into the agar to mark origin of cells 1 through 4); colony forming capacity of single cells (A4.1 is circled in yellow). B) Ploidy of colonies derived from single-cell clones (see Dataset S1 for histograms), named for the coordinate of the parent strain in the evolved 96-well plate and the isolate number. C) Mutation rate measurements of haploid cultures as determined by fluctuation analysis of canavanine resistance (Can^R). Error bars represent 95% confidence intervals. (See Dataset S1 for Table of values.)

Figure S3. Frequency of mating-type switching and same-sex mating in mutator cells.



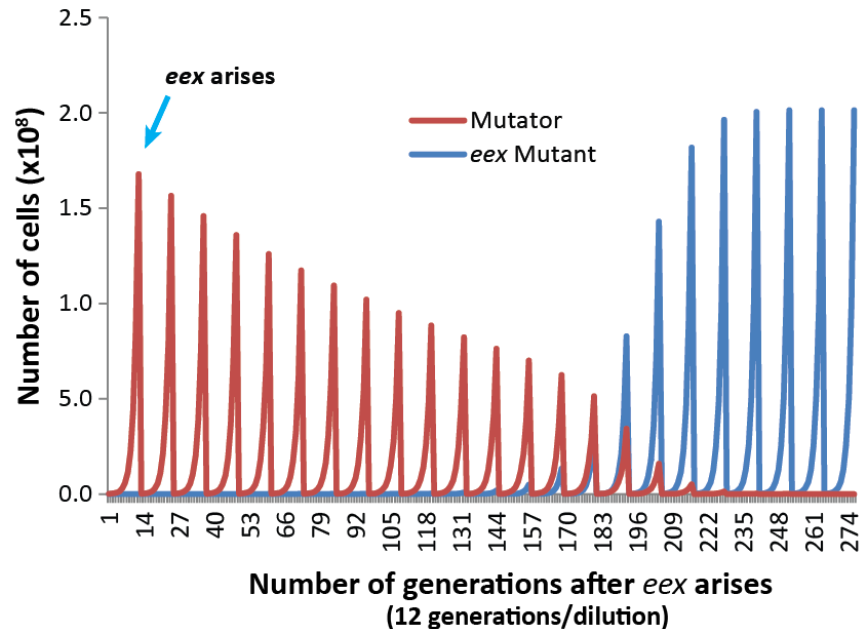
A) Experimental design. Same sex haploid cultures with opposite *CAN1* alleles (*CAN1::natMX*, *can1Δ::HIS3*) were mixed and plated for *CAN1::natMX/can1Δ::HIS3* diploids. B) Summary of flow cytometry and mating-type PCR assays of colonies resulting from the crosses indicated in the white boxes. The mutator cultures used for each cross are indicated by their 96-well coordinate (see Figure 1). The color of the box indicates ploidy. Blue 1n boxes are haploids included as controls (see Dataset S1 for individual histograms). Results of Mating type PCR: α , *MAT α* ; a , *MAT a* C) Mating-type PCR gels.

Figure S4. Frequency of mating-type switching and same-sex mating in wild-type cells.



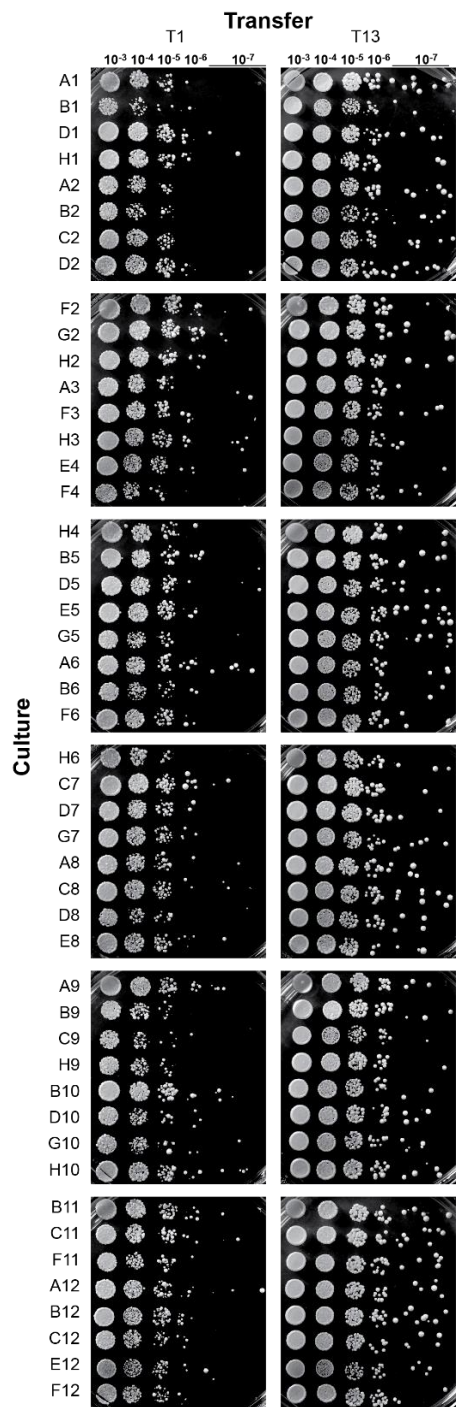
A) Experimental design. Same sex haploid colonies with opposite *CAN1* alleles (*CAN1::natMX*, *can1Δ::HIS3*) were mixed, incubated in media, and plated for *CAN1::natMX/can1Δ::HIS3* diploids. B) Frequencies of His⁺ NTC^R colonies per 10^7 cells. C) Summary of flow cytometry and mating-type PCR assays of colonies resulting from *MATα* x *MATα* matings. The color of the box indicates ploidy (see Dataset S1 for individual histograms). D) Summary of flow cytometry and mating-type PCR assays of colonies resulting from *MATa* x *MATa* matings. AH4002, AH4003, AH4010 represent haploid strains; 2 x 15 and 3 x 10 are *MATa/α* control diploids derived from matings between AH4002 x AH4015 and AH4003 x AH4010.

Figure S5. Simulation of *eex* adaption during diploid mutator evolution.



Exponential growth of *pol3-01/pol3-01 msh6Δ/msh6Δ* cells (Mutator, red line) and an *eex* mutant (blue line) with a 10-fold lower mutation rate were modeled assuming the only limiting factor for growth was homozygous inactivation of essential genes (see Dataset S1 for calculations). Each peak models a 1:500 dilution of the culture from $\sim 10^8$ cells to $\sim 10^5$ cells.

Figure S6. Colony forming capacity of evolved *pol3-01/pol3-01 msh6Δ/msh6Δ* cultures.



Ten-fold serial dilutions from overnight cultures were plated on SC plates and incubated for two days at 30°C. T1 and T13 refer to first and thirteenth sub-culturing steps after the initial inoculations. The culture designation on the left refers to the position of the culture in the 96 well plate (see Figure 3).

Figure S7. Mutation spectra and phylogenetic relationships of evolved *pol3-01/pol3-01 msh6Δ/msh6Δ* T25 subclones.

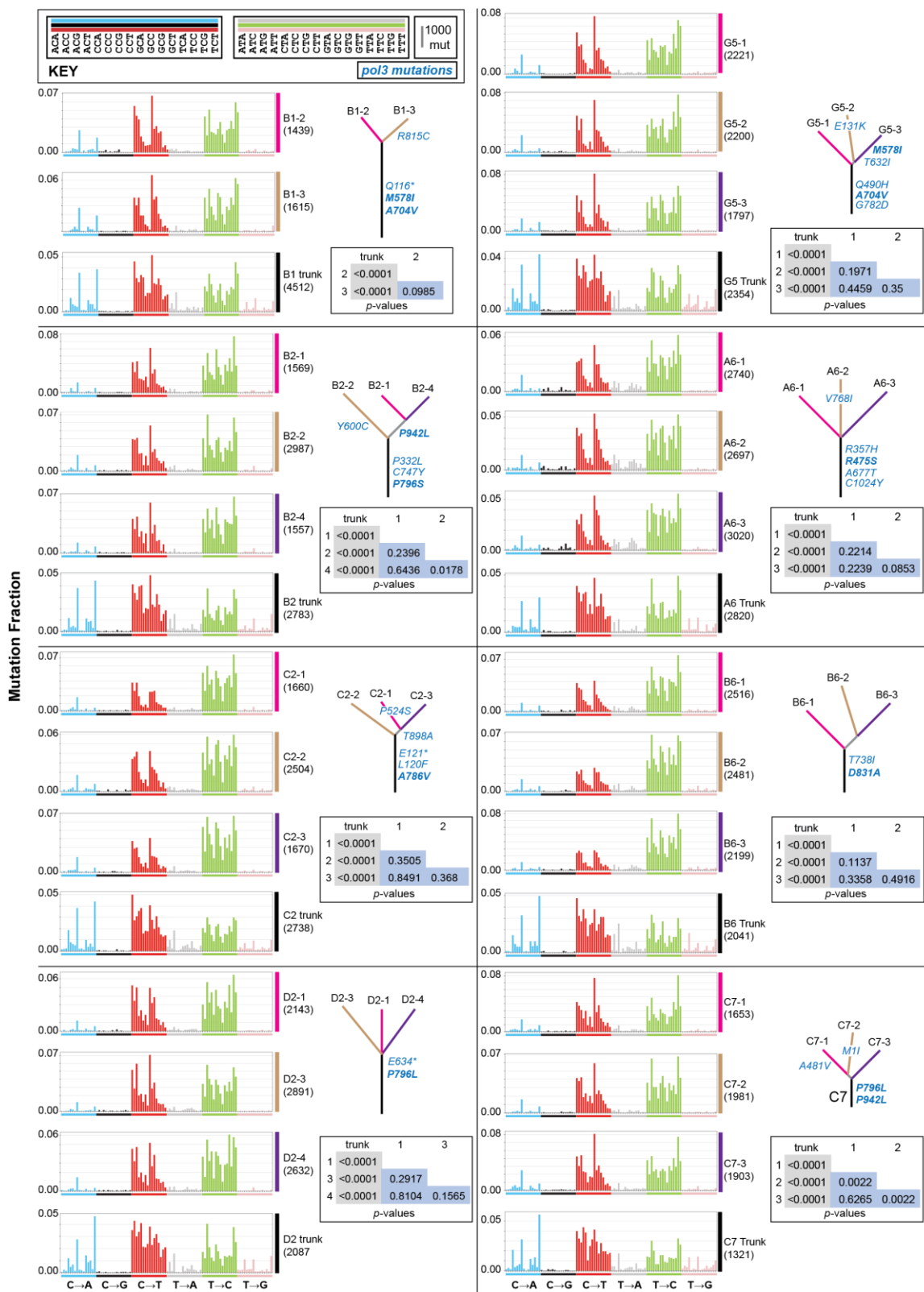
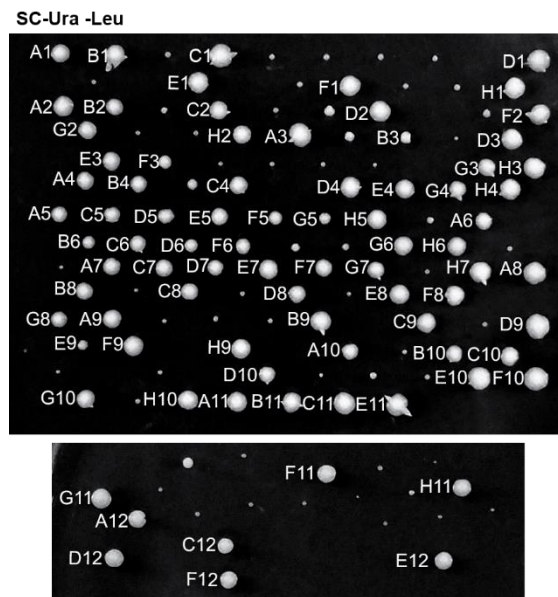


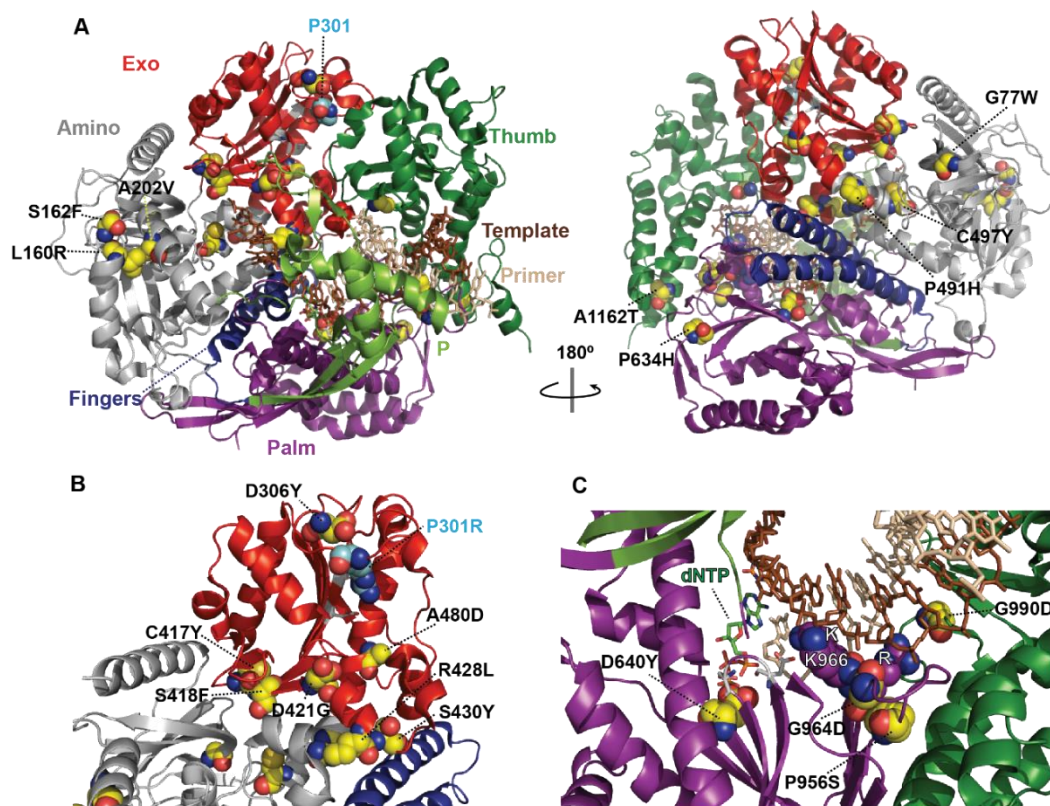
Figure S7, continued. Mutational variants identified by whole genome sequencing of subclones isolated from different evolved cultures were classified as shared (trunk) and unique. The nucleotide context 5' and 3' of each mutational site (represented as the pyrimidine base T or C) were used to classify the 6 mutation types (C:G→A:T, C:G→G:C, C:G→T:A, T:A→A:T, T:A→C:G, T:A→G:C) into 96 trinucleotide contexts. Each mutation type family is color-coded (see Key for color and context order). The bar height for mutation type represents the fraction of the total mutations (to the right of each plot). Phylogenetic trees: line length corresponds to the number of mutations, line color corresponds to mutation spectra, observed *pol3* mutations are in blue lettering (bold represents known or likely antimutators). Inset tables: *p*-values determined by the hypergeometric test.

Figure S8. Growth phenotypes of *pol2-P301R/POL2 msh2Δ/msh2Δ* and *pol2-P301R/pol2-P301R msh2Δ/msh2Δ* zygotes.



Zygote colonies were isolated, as described in Figure 5, on synthetic complete media lacking uracil and leucine (SC-Ura-Leu) by mating cells dissected from tetrads of AH11304 (*URA3::pol2-P301R/POL2 msh2Δ::LEU2/MSH2*). Each colony used for the evolution experiment in Figure 5 is labeled to the left by the 96-well coordinate position. Small, unlabeled colonies are derived from *pol2-P301R/pol2-P301R msh2Δ/msh2Δ* zygotes and were not evolved.

Figure S9. Locations of amino acid substitutions encoded by *pol2-P301R* mutator suppressors.



A) Two orientations of the wild-type *S. cerevisiae* Polε structure (Protein database accession code 4M80 (Swan *et al.* 2009)) are shown as ribbon diagrams of the α-carbon backbone (rendered in PyMol). Structural domains are color coded as follows: Amino (gray), Exo (red), processivity (P) (chartreuse), Palm (purple), Fingers (blue) and Thumb (green). Yellow spheres correspond to amino acid substitutions encoded by mutator suppressors. The incoming dNTP is denoted by green CPK sticks. The primer DNA is represented by tan sticks and the template DNA, by brown sticks. Active-site carboxylate side chains are gray CPK sticks coming out of the purple (palm) or red (exo) ribbons. L160R, S162F, and A202V affect interacting residues that play a structural role in the amino terminal domain in a region not previously implicated in fidelity. B) Locations of exo substitutions within the Exo domain of the Pol2p-P301R mutant polymerase (Protein database accession code 6i8a (Parkash *et al.* 2019)), which may be candidates for enhancing proofreading function. C) Substitutions positioned to influence dNTP binding and the KKRYA Motif. D640 is 3.21 Å and 3.46 Å from the γ and α-phosphates of the incoming dNTP, respectively. K966, K967(K), and R968(R) from the KKRYA motif, which monitors the minor groove for non-Watson-Crick base-pairing, are depicted as purple CPK space-filling spheres. We previously isolated an antimutator allele affecting K966 (*pol2-K966Q*) (Williams *et al.* 2013). P956S is 3.23 Å from the primary amino group of R968.

Table S1: Similarity of the *pol2/POL2 msh2Δ/msh2Δ* mutation spectra to mutation signatures in cancer.

Signature	Cosine Similarity
SBS1	0.138
SBS2	0.178
SBS3	0.485
SBS4	0.483
SBS5	0.537
SBS6	0.239
SBS7a	0.191
SBS7b	0.209
SBS7c	0.175
SBS7d	0.218
SBS8	0.519
SBS9	0.456
SBS10a	0.634
SBS10b	0.149
SBS11	0.344
SBS12	0.233
SBS13	0.070
SBS14	0.793
SBS15	0.217
SBS16	0.276
SBS17a	0.053
SBS17b	0.092
SBS18	0.626
SBS19	0.301
SBS20	0.536
SBS21	0.238
SBS22	0.046
SBS23	0.299
SBS24	0.333
SBS25	0.447
SBS26	0.236
SBS27	0.140
SBS28	0.159
SBS29	0.472
SBS30	0.340
SBS31	0.258
SBS32	0.501
SBS33	0.149
SBS34	0.075
SBS35	0.424
SBS36	0.701
SBS37	0.276
SBS38	0.317
SBS39	0.241
SBS40	0.623
SBS41	0.304
SBS42	0.453
SBS43	0.052
SBS44	0.561
SBS45	0.396
SBS46	0.266
SBS47	0.201
SBS48	0.026
SBS49	0.071
SBS50	0.282
SBS51	0.212
SBS52	0.180
SBS53	0.128
SBS54	0.144
SBS55	0.082
SBS56	0.653
SBS57	0.370
SBS58	0.375
SBS59	0.322
SBS60	0.025

Dataset S1. Flow cytometry, mutation rates, and modeling of diploid evolution.	
Page	Description
1	Ploidy measurements of eex mapping strains described in S1B Fig.
2	Ploidy measurements of <i>pol2-4 msh6Δ</i> evolved cultures described in Fig 1B.
3	Ploidy measurements of <i>pol2-4 msh6Δ</i> T8 subclones described in Fig 1C.
4	Ploidy measurements of <i>pol2-4 msh6Δ</i> subclones described in S2A Fig.
5	Mutation rate measurements of <i>pol2-4 msh6Δ</i> subclones described in S2B Fig.
6	Ploidy measurements of strains isolated by same sex mating between T1 <i>pol2-4 msh6Δ</i> cultures described in S3 Fig.
7	Ploidy measurements of competition experiment between <i>pol2-4 msh6Δ</i> derived diploid and tetraploid strains described in Fig 2B.
8	Simulation of evolution of <i>pol3-01/pol3-01 msh6Δ/msh6Δ</i> evolved cultures described in S4 Fig.
9	Ploidy measurements of <i>pol3-01/pol3-01 msh6Δ/msh6Δ</i> evolved cultures described in Fig 3B.
10	Ploidy measurements of T25 <i>pol3-01/pol3-01 msh6Δ/msh6Δ</i> subclones analyzed in Fig 4
11	Mutation rate measurements of T25 <i>pol3-01/pol3-01 msh6Δ/msh6Δ</i> subclones described in Fig 4.
12	Ploidy measurements of <i>pol2-P301R/POL2 msh2Δ/msh2Δ</i> evolved cultures described in Fig.5C.
13	Mutation rate measurements of T10 <i>pol2-P301R/POL2 msh2Δ/msh2Δ</i> subclones described in Fig. 5D and <i>pol2</i> changes in Fig.5E.
14	POLE-P286R cancers on cBioPortal depicted in Fig. 5G.

Dataset S2. Whole genome sequencing.	
Page	Description
1	AH164_B1_SNPs: Sequencing coverage, evolutionary relationships, distribution of variant allele frequencies (VAF), and annotation of SNPs for AH164_B1 <i>pol3-01/pol3-01 msh6Δ/msh6Δ</i> subclones.
2	AH164_B1_Indels: Sequencing coverage, evolutionary relationships, and annotation of Indels for AH164_B1 <i>pol3-01/pol3-01 msh6Δ/msh6Δ</i> subclones.

3	AH164_B2_SNPs: Sequencing coverage, evolutionary relationships, distribution of VAFs, and annotation of SNPs for AH164_B2 <i>pol3-01/pol3-01 msh6Δ/msh6Δ</i> subclones.
4	AH164_B2_Indels: Sequencing coverage, evolutionary relationships, and annotation of Indels for AH164_B2 <i>pol3-01/pol3-01 msh6Δ/msh6Δ</i> subclones.
5	AH164_C2_SNPs: Sequencing coverage, evolutionary relationships, distribution of VAFs, and annotation of SNPs for AH164_C2 <i>pol3-01/pol3-01 msh6Δ/msh6Δ</i> subclones.
6	AH164_C2_Indels: Sequencing coverage, evolutionary relationships, and annotation of Indels for AH164_C2 <i>pol3-01/pol3-01 msh6Δ/msh6Δ</i> subclones.
7	AH164_D2_SNPs: Sequencing coverage, evolutionary relationships, distribution of VAFs, and annotation of SNPs for AH164_D2 <i>pol3-01/pol3-01 msh6Δ/msh6Δ</i> subclones.
8	AH164_D2_Indels: Sequencing coverage, evolutionary relationships, and annotation of Indels for AH164_D2 <i>pol3-01/pol3-01 msh6Δ/msh6Δ</i> subclones.
9	AH164_G5_SNPs: Sequencing coverage, evolutionary relationships, distribution of VAFs, and annotation of SNPs for AH164_G5 <i>pol3-01/pol3-01 msh6Δ/msh6Δ</i> subclones.
10	AH164_G5_Indels: Sequencing coverage, evolutionary relationships, and annotation of Indels for AH164_G5 <i>pol3-01/pol3-01 msh6Δ/msh6Δ</i> subclones.
11	AH164_A6_SNPs: Sequencing coverage, evolutionary relationships, distribution of VAFs, and annotation of SNPs for AH164_A6 <i>pol3-01/pol3-01 msh6Δ/msh6Δ</i> subclones.
12	AH164_A6_Indels: Sequencing coverage, evolutionary relationships, and annotation of Indels for AH164_A6 <i>pol3-01/pol3-01 msh6Δ/msh6Δ</i> subclones.
13	AH164_B6_SNPs: Sequencing coverage, evolutionary relationships, distribution of VAFs, and annotation of SNPs for AH164_B6 <i>pol3-01/pol3-01 msh6Δ/msh6Δ</i> subclones.

14	AH164_B6_Indels: Sequencing coverage, evolutionary relationships, and annotation of Indels for AH164_B6 <i>pol3-01/pol3-01 msh6Δ/msh6Δ</i> subclones.
15	AH164_C7_SNPs: Sequencing coverage, evolutionary relationships, distribution of VAFs, and annotation of SNPs for AH164_C7 <i>pol3-01/pol3-01 msh6Δ/msh6Δ</i> subclones.
16	AH164_C7_Indels: Sequencing coverage, evolutionary relationships, and annotation of Indels for AH164_C7 <i>pol3-01/pol3-01 msh6Δ/msh6Δ</i> subclones.
17	Table of cosine similarity and hypergeometric tests of similarity between <i>pol3-01/pol3-01 msh6Δ/msh6Δ</i> mutation spectra.
18	Output of dNdScv analysis of AH164 evolved cultures reported in Figure 4E.
19	Evolutionary relationships, variant counts, and annotated <i>pol2</i> variants for <i>pol2-P301R/POL2 msh2Δ/msh2Δ</i> evolved strains used for Figure 5E.
20	Annotations of all variants in <i>pol2-P301R/POL2 msh2Δ/msh2Δ</i> evolved strains described in Figure 5.
21	Table of cosine similarity and hypergeometric tests of similarity between <i>pol2-P301R/POL2 msh2Δ/msh2Δ</i> mutation spectra.